HHS Public Access

Author manuscript

Nat Med. Author manuscript; available in PMC 2013 October 01.

Published in final edited form as:

Nat Med. 2013 April ; 19(4): 465–472. doi:10.1038/nm.3105.

Persistent antigen at vaccination sites induces tumor-specific CD8+ T cell sequestration, dysfunction and deletion

Yared Hailemichael[1], **Zhimin Dai**[1], **Nina Jaffarzad**[1], **Yang Ye**[1], **Miguel A Medina**[1], **Xue-Fei Huang**[1], **Stephanie M Dorta-Estremera**[1], **Nathaniel R Greeley**[1], **Giovanni Nitti**[1], **Weiyi Peng**[1], **Chengwen Liu**[1], **Yanyan Lou**[1], **Zhiqiang Wang**[2], **Wencai Ma**[2], **Brian Rabinovich**[1], **Kimberly S Schluns**[3], **Richard E Davis**[2], **Patrick Hwu**[1], and **Willem W Overwijk**[1]

[1]Department of Melanoma Medical Oncology, The University of Texas M.D. Anderson Cancer Center, Houston, TX

[2]Department of Lymphoma/Myeloma, The University of Texas M.D. Anderson Cancer Center, Houston, TX

[3]Department of Immunology, The University of Texas M.D. Anderson Cancer Center, Houston, TX

Abstract

To understand why cancer vaccine-induced T cells often fail to eradicate tumors, we studied immune responses in mice vaccinated with gp100 melanoma peptide in incomplete Freund's adjuvant (IFA), commonly used in clinical cancer vaccine trials. Peptide/IFA vaccination primed tumor-specific $CD8^+$ T cells, which accumulated not in tumors but at the persisting, antigen-rich vaccination site. Once there, primed T cells became dysfunctional and underwent antigen-driven, Interferon-γ (IFN-γ) and Fas ligand (FasL)-mediated apoptosis, resulting in hyporesponsiveness to subsequent vaccination. Provision of anti-CD40 antibody, Toll-like receptor 7 (TLR7) agonist and interleukin-2 (IL-2) reduced T cell apoptosis but did not prevent vaccination site sequestration. A non-persisting vaccine formulation shifted T cell localization towards tumors, inducing superior anti-tumor activity while reducing systemic T cell dysfunction and promoting memory formation. Persisting peptide/IFA vaccine depots can induce specific T cell sequestration, dysfunction and deletion at vaccination sites; short-lived formulations may overcome these limitations and result in greater therapeutic efficacy of peptide-based cancer vaccines.

Cancer vaccines have shown objective therapeutic benefit in several recent randomized clinical trials[1-5], but a pressing question remains why many vaccinated cancer patients show increased levels of circulating tumor-specific T cells without tumor regression[6]. A host of

AUTHOR CONTRIBUTION

Y.H. designed and performed experiments and wrote the manuscript. Z.D., N.J., Y.Y., M.M., X.F.H., N.G., G.N., S.M.D., W.P., C.W.L and Y.L. performed experiments. K.S. constructed VSV.gp100. B.R. and P.H. provided v-effLuc-GFP expressing retroviral construct and imaging expertise. Z.W., W.M and R.E.D. performed and analyzed Gene Expression Arrays. W.W.O. conceived the study and wrote the manuscript.

COMPETING FINANCIAL INTERESTS

The authors declare no competing financial interests.

clinical trials has employed minimal determinant peptides formulated in IFA to induce tumor-specific T cell responses in cancer patients. Typically, antigen-specific T cell responses were induced; however objective anti-tumor responses have been rare[7]. A recent prospective randomized multi-center phase III trial showed that vaccination of melanoma patients with a melanocyte differentiation antigen-derived gp100 peptide emulsified in IFA doubled the objective response rate to high-dose IL-2 therapy and increased progression-free survival, however increased gp100-specific $CD8^+$ T cell responses in peripheral blood did not necessarily result in tumor shrinkage[1].

While many mechanisms of immune regulation, suppression and escape can permit tumor growth despite tumor-specific $CD8^+$ T cell responses[8, 9], it is also possible that IFA-based cancer vaccines have inherent properties that limit their clinical efficacy. IFA-based vaccines are water-in-oil emulsions of antigen in mineral oil and mannide monooleate as a surfactant[10]. IFA is thought to induce local inflammation and form a depot that protects antigen from degradation and slowly releases it to antigen presenting cells (APCs)[11, 12]. Vaccination of animals with synthetic MHC Class I-restricted minimal determinant peptides in IFA often stimulates $CD8^+$ T cell responses but sometimes inhibits them[1314], possibly due to systemic peptide presentation by non-professional APCs[13-15]. Overall, $CD8^+$ T cell responses after peptide/IFA vaccination are poorly understood, yet 98 federally registered clinical trials of IFA-based cancer vaccines have been completed in the USA alone, and 37 additional trials are actively enrolling cancer patients at this moment[16]. Here, we used a preclinical model to study melanoma-specific $CD8^+$ T cell immune responses after gp100/IFA vaccination.

RESULTS

Gp100/IFA vaccination induces $CD8^+$ T cell hyporesponsiveness

To study the fate of melanoma-specific $CD8^+$ T cells after peptide vaccination, we tracked T cell receptor-transgenic pmel-1 T cells in mice vaccinated with heteroclitic $gp100_{25\text{-}33}$ peptide emulsified in IFA[17-19]. While gp100/IFA induced significant expansion of pmel-1 T cells, their levels dropped to near-undetectable by 3 weeks and did not rebound after viral boosting with VSV.gp100 (Fig. 1a). Vaccination with VSV.gp100 and gp100/IFA induced similar pmel-1 T cell peak levels, but while VSV.gp100-induced pmel-1 T cell responses persisted, gp100/IFA responses fell precipitously and did not result in substantial memory (Fig. 1b). Combination immunization with VSV.gp100 and gp100/IFA induced similarly short-lived T cell responses, suggesting that peptide/IFA vaccination dominantly destroyed long-lived CD8 T cell immunity. Indeed, even 30 d after VSV.gp100 vaccination, gp100/IFA vaccination resulted in brief pmel-1 T cell expansion followed by dramatic termination of established T cell memory (Fig. 1b and Supplementary Fig. 1). Similar responses to peptide/IFA vaccination were observed for endogenous $CD8^+$ T cells specific for chicken ovalbumin $OVA_{257\text{-}264}$ (Fig. 1c) and $OVA_{257\text{-}264}$-specific OT-I T cells (Supplementary Fig. 2a)[15, 20] as well as OT-II $CD4^+$ T cells after $OVA_{323–339}$ peptide vaccination (Supplementary Fig. 2b), suggesting vaccination-induced hyporesponsiveness was not a peculiarity of the gp100 peptide or of pmel-1 T cells. We found no optimal dose of antigen that primed T cells without subsequent hyporesponsiveness; the lowest dose of

gp100 peptide that could induce pmel-1 T cell priming (10 μg) still induced subsequent hyporesponsiveness, arguing against classical high-zone tolerance (Supplementary Fig. 3)[21, 22].

Gp100 peptide was presented on $CD11c^+$ DCs and $CD19^+$ B cells in the vaccine-draining lymph node (VdLN), as previously reported for OVA peptide[15, 21] (Supplementary Fig. 4a). B cell-deficient Igh-KO mice and CD4-KO mice were not protected from gp100/IFA-induced hyporesponsiveness (Supplementary Fig. 4b), indicating that B cells and $CD4^+$ Tregs were not main mediators of gp100/IFA-induced hyporesponsiveness.

Persistent antigen presentation drives T cell accumulation

To extend our analysis of vaccination-induced T cells beyond the blood compartment, we visualized luciferase gene-transduced pmel-1 T cells[23] transferred to vaccinated mice bearing gp100-expressing B16 melanoma. Mice vaccinated with VSV.gp100 showed robust pmel-1 T cell levels in blood and efficient accumulation in tumors (Fig. 1d). Remarkably, in mice receiving both VSV.gp100 and gp100.IFA vaccination, pmel-1 T cells were also found in the circulation but largely accumulated at gp100/IFA vaccination sites and VdLN, and only slightly at the tumor site (Fig. 1d). T cell localization to the gp100/IFA vaccination site and the VdLN was dependent on presence of cognate gp100 antigen as it did not occur at antigen-free saline/IFA control sites (Fig. 1e). Flow cytometric evaluation of B16 tumor-bearing mice receiving naive pmel-1 T cells and gp100/IFA vaccination gave similar results (Supplementary Fig. 5).

Since T cell accumulation at vaccination sites was antigen-driven (Fig. 1e), we examined how long gp100/IFA vaccine depots could exert this effect. Pmel-1 effector T cells preferentially accumulated at fresh and 30 d old gp100/IFA vaccine depots compared to palpable B16 tumors or antigen-negative saline/IFA depots (Fig. 2a). Persistent local peptide presentation[11, 12, 15, 24] was observed in VdLN but not spleen 30 d after gp100/IFA vaccination (Fig. 2b). Remarkably, 96 d old gp100/IFA vaccine depots were still able to induce expansion of freshly injected naive pmel-1 T cells (Fig. 2c). Similarly, the HLA-A0201-binding, human $gp100_{209\text{-}217(210M)}$ peptide emulsified in clinical grade IFA (Montanide ISA-51 VG), commonly used to vaccinate melanoma patients[1, 6], was persistently presented on APCs in the VdLN of HLA-A0201-Tg mice (Supplementary Fig. 6).

IFN-γ and FasL mediate T cell apoptosis at the vaccination site

We next determined whether vaccination-induced T cell hyporesponsiveness was due to the prolonged interaction between pmel-1 T cells and persistent gp100 peptide at the vaccination site. Pmel-1 T cells which productively interacted with gp100/IFA for only 48 h expanded in response to subsequent vaccination, while pmel-1 T cells exposed to gp100/IFA for 5 d (Supplementary Fig. 7) or 30 d (Fig. 3a) did not. Vaccination-induced hyporesponsiveness correlated with increased apoptotic death of pmel-1 T cells from gp100/IFA VdLN or vaccination sites (Fig. 3b). Upon transfer of mixed OT-I and pmel-1 effector T cells we observed >15-fold increase in apoptotic death in pmel-1 T cells *vs.* their OT-I counterparts at gp100/IFA vaccination sites (Supplementary Fig. 8a), suggesting T cell

apoptosis required TCR engagement. To investigate the role of TCR signaling strength on deletion[25, 26], we transferred OT-I T cells and vaccinated with the cognate OT-I ligand, SIINFEKL, or the altered ligand, SIITFEKL, which displays similar binding to H-2K^b MHC Class I molecules but has a much lower affinity for the OT-I TCR[27]. SIINFEKL-primed OT-I T cells expanded faster and to greater numbers than SIITFEKL-primed OT-I T cells as reported[27], but apoptotic death at the vaccination site was similar (Supplementary Fig. 9a,b).

Expression of the death receptor, Fas/CD95[28], was increased on pmel-1 T cells at the gp100/IFA vaccination site but not in spleen and blood (Fig. 3c). In mice deficient in Fas ligand/CD95L (FasL), pmel-1 T cell apoptosis at the gp100/IFA vaccination site was reduced (Fig. 3d). Endogenous, OVA-specific CD8$^+$ T cells in OVA/IFA-vaccinated mice deficient in IFN-γ, a known inducer of Fas, FasL and T cell apoptosis[29], showed decreased Fas expression and T cell apoptosis, and increased T cell numbers at the vaccination site (Fig. 3e,f). Host cells that could mediate this T cell death induced by IFN-γ and Fas/FasL include immunoregulatory myeloid cells[30, 31]. At gp100/IFA vaccination sites, IFN-γ promoted accumulation of CD11b$^+$Gr-1^{hi}Ly6C^{int} cells resembling granulocytic myeloid derived suppressor cells (MDSCs), and of CD11b$^+$Gr-1^{int}Ly6C^{hi} cells, resembling monocytic MDSCs, recently reported as particularly immunosuppressive in spleens from tumor-bearing hosts[32] (Supplementary Fig. 10a). The latter cell subset showed marked IFN-γ-driven upregulation of FasL and the immunosuppressive PD-1 ligand, PD-L1 (Supplementary Fig. 10a,b). Together with the reported near-complete recruitment of the systemic antigen-specific T cell pool to sites of vaccination[33], these data suggest that gp100/IFA vaccination induced antigen-driven recruitment of the majority of gp100-specific T cells to the VdLN/vaccination site, where they underwent priming followed by antigen-driven apoptosis mediated by IFN-γ and FasL in a T cell-hostile environment replete with myeloid cells expressing FasL and PD-L1.

Short-lived vaccine formulation induces strong T cell responses

Since pmel-1 T cells could be rescued from apoptosis by limiting their exposure to gp100/IFA vaccine depots, we tested the reverse, more clinically applicable approach of limiting the persistence of vaccine depots. Simply replacing non-biodegradable IFA with saline abolished gp100 peptide presentation in VdLN within 7 d after vaccination with gp100/saline (Fig. 4a), but also abolished pmel-1 T cell priming (Fig. 4b). We then added 3 immunostimulatory molecules, hereafter referred to as “covax”, known to enhance peptide vaccination by licensing and activating APCs (anti-CD40 mAb[34, 35] and the TLR7 agonist imiquimod[36, 37]) and directly supporting primed CD8$^+$ T cells (Interleukin-2)[18, 38]. Gp100/saline/covax vaccination induced strong, boostable pmel-1 T cell expansion without hyporesponsiveness (Fig. 4b,c).

Addition of covax allowed more T cell persistence after gp100/IFA vaccination, although post-peak apoptosis and contraction were still stronger after IFA *vs.* saline-based vaccination (Fig. 4c,d). Apoptosis correlated with downregulation of CD127/IL-7Rα and antiapoptotic Bcl-2 and Bcl-xL and upregulation of proapoptotic Bim/Bcl-2L11 in T cells induced with gp100/IFA *vs.* gp100/saline, consistent with the reported involvement of CD127-controlled Bcl-2 family members in antigen-driven T cell death[39-41] (Fig. 4e and Supplementary Figs.

17b **and** 18). Even after addition of covax, antigen presentation in VdLN after saline-based vaccination all but vanished by 6 d, while antigen presentation after IFA-based vaccination actually increased over time (Supplementary Fig. 11).

Short-lived vaccine promotes T cell localization to tumor

While gp100/IFA/covax and gp100/saline/covax both induced high levels of pmel-1 T cells in the blood, suppression of melanoma growth was stronger after vaccination with gp100/saline/covax (Fig. 4f). Similar results were seen after therapy of established, palpable melanomas (Fig. 4g) and after priming with VSV.gp100 and boosting with gp100/saline/covax *vs.* gp100/IFA/covax (Supplementary Fig. 12). Saline-based vaccination induced preferential T cell localization and tissue destruction at the tumor site, while IFA-based vaccination induced the reverse pattern of T cell sequestration, local tissue destruction and killing of normal $gp100^+$ pigment cells (vitiligo) at the vaccination site (Fig. 5a,b **and** Supplementary Fig. 13). Similar results were obtained with OVA antigen, a model for non-self antigens such as viral and mutated gene products[3, 42] (Supplementary Fig. 14). Since a recent clinical trial[3] showed promising therapeutic activity of vaccination with elongated ("long") peptides in IFA, we compared antigen presentation, T cell responses, sequestration and anti-tumor activity after vaccination with short (9 aa) and long (20 aa) gp100 peptide in IFA. Compared to short peptide, long peptide induced minimal T cell sequestration at the vaccination site, no rapid contraction of the T cell response, and superior anti-tumor activity (Supplementary Fig. 15a-c). Long gp100 peptide was presented only by relatively rare DCs in the vaccine-draining lymph node (VdLN), while short gp100 peptide was presented by multiple VdLN cell types including ubiquitous B cells (Supplementary Fig. 15d). Since long peptides require trimming by DC-specific intracellular enzymes to allow efficient binding to MHC class I molecules[15], the resulting DC-specific antigen presentation possibly reduced the intensity of local chronic antigen presentation and consequent T cell sequestration and deletion[28].

Since chemokines mediate T cell localization[43], we studied chemokines at vaccination sites and tumors. CXCR3 and its ligands, CXCL9 and CXCL10 are dominant drivers of $CD8^+$ effector T cell trafficking, and effector pmel-1 T cells from vaccinated mice expressed high levels of CXCR3 (Fig. 5c). CXCL9 and CXCL10 were present at gp100/IFA but not gp100/saline vaccination sites, and at tumor sites 6 d after vaccination (Fig. 5d). IFN-γ, a major inducer of CXCL9/10, was also detected at the gp100/IFA but not saline/IFA or gp100/saline vaccination site, suggesting it was produced by pmel-1 T cells in response to persistent gp100 peptide (Fig. 5d **and** 6c). Interestingly, the gp100/IFA vaccination site also uniquely contained IL-1β, IL-6 and IL-17, suggesting a local Type 17 immune response that did not, however, extend to the tumor (Fig. 5d **and** Supplemental Fig. 16).

Short-lived vaccine prevents T cell dysfunction

We examined whether persistent gp100 antigen affected pmel-1 T cell function as observed in settings of chronic viral infection and cancer[44, 45]. Compared to gp100/saline/covax, gp100/IFA/covax induced stronger upregulation of genes associated with proliferation (Supplementary Fig. 17a), apoptosis (Supplementary Fig. 17b),effector differentiation (Supplementary Fig. 17c) and memory formation (Fig. 6a, Supplementary Fig. 17d **and**

18)[34], in line with our earlier findings (Fig. 4). Gp100/IFA/covax-primed pmel-1 T cells in blood showed upregulation of inhibitory receptors PD-1 and to a lesser extent LAG-3 and Tim-3 (HAVCR2) during the first 21 d, while memory markers CD127 and CD62L remained low; this pattern was reversed after vaccination with gp100/saline/covax (Fig. 6b). At the vaccination site, gp100/IFA/covax induced higher, antigen-driven expression of inhibitory receptors PD-1, LAG-3, CTLA-4 and Tim-3 (Fig. 6c **and** Supplementary Fig. 8b) and dysfunction as measured by decreased IFN-γ and TNF-α production suggestive of partial exhaustion (Fig. 6c)[45, 46]. Eventually (d 80), remaining gp100/IFA-primed pmel-1 T cells exhibited a predominant effector ($CD127^{lo}/CD62L^{lo}$) and effector memory phenotype ($CD127^{hi}/CD62L^{lo}$), while gp100/saline-primed cells largely displayed a central memory phenotype ($CD127^{hi}/CD62L^{hi}$) (Supplementary Fig. 19).

Altogether, persistent antigen at vaccination sites induced priming of tumor-specific T cells followed by their sequestration, dysfunction and deletion. Strong proimmunogenic signals could partially overcome T cell deletion, but could not overcome local antigen-driven chemokine induction, T cell sequestration and dysfunction and tissue destruction at vaccination sites. In contrast, a short-lived vaccine formulation induced long-lived, functional T cells that localized preferentially to tumor sites, increasing anti-tumor activity.

DISCUSSION

We found that persistent gp100/IFA vaccine depots induced priming of tumor-specific $CD8^+$ T cells which accumulated at the vaccination site, preventing their tumor localization while causing their dysfunction and deletion. Different peptides in IFA display different pharmacokinetics and *in vivo* distribution[13, 14, 47, 48]. We found prolonged local release from IFA depots of the 3 peptides examined in this study: H-$2D^b$-restricted mouse heteroclitic (h)$gp100_{25\text{-}33}$, H-$2K^b$-restricted chicken $ovalbumin_{257\text{-}264}$ and HLA-A*0201-restricted human heteroclitic $gp100_{209\text{-}217(210M)}$. Clinical observations suggest that sequestration and deletion of primed T cells can also occur in cancer patients vaccinated with minimal determinant peptides in IFA. Tumor-specific $CD8^+$ T cells were deleted after vaccination of cancer patients with leukemia antigen-derived WT-1 and PR1 peptides in IFA[49]. Vaccination of melanoma patients with heteroclitic MART-1 peptide in IFA combined with the TLR9 agonist, CpG, induced re-inflammation of distant, old MART-1/IFA/CpG vaccination sites, poor tumor localization and no tumor regression[50, 51]. Similar inflammation of old vaccination sites after revaccination was observed in patients with cervical cancer vaccinated with HPV peptides in IFA[52] and in patients with colorectal and ovarian cancer vaccinated with p53-derived peptides in IFA[53, 54]. The latter study also showed specific T cell accumulation at vaccination sites and no tumor regression. Finally, patients vaccinated with multiple melanoma-derived peptides in IFA showed accumulation of primed $CD8^+$ T cells in VdLN that exceeded accumulation at tumor sites[55, 56]. We speculate that in this series of clinical trials, low numbers of T cells surviving earlier vaccination expanded upon revaccination and localized to and inflamed both new and old, persisting, peptide-rich vaccination sites but not tumor sites.

A limitation of our animal model is the difference in body size between a mouse and human relative to antigen dose and vaccine depot size. We never found a gp100 peptide dose that

was “just right” to induce priming without subsequent T cell deletion. Since persistent gp100 antigen presentation was restricted to the vaccination site and VdLN, body size does not appear to be a major confounding factor in this study.

Importantly, our data indicate that vaccination with peptide in IFA is superior to no vaccination, since some primed T cells still reach the tumor site. A recent randomized phase III study[1] showed modest but real clinical benefit of peptide vaccination when added to high-dose IL-2 therapy, possibly because IL-2 induces systemic cytokine release that can activate APCs and support vaccine-primed T cell survival, similar to covax in our study. However, our findings suggest that the full therapeutic power of current IFA-based vaccine therapy may not be realized due to vaccination site sequestration, dysfunction and deletion of most primed T cells. In one study, vaccination with $gp100_{209\text{-}217(210M)}$ peptide in IFA raised gp100-specific $CD8^+$ T cell levels to >1% of peripheral $CD8^+$ T cells in the majority of melanoma patients, although this required up to 64 vaccinations over 48 weeks[6]. Again, gp100-specific $CD8^+$ T cell levels in blood did not predict clinical benefit while significant local vaccination site toxicity was observed that caused 17% of vaccinated patients to withdraw from the study[6]. Interestingly, a recent trial of vaccination of healthy volunteers with HIV-derived peptides in IFA had to be discontinued because of ulcerating sterile inflammation and abscesses at vaccination sites that increased in severity with the intensity of the induced specific T cell response[56].

We propose that IFA-based vaccination turns the vaccination site into a persistent source of T cell priming as well as a target tissue, in a vicious cycle where T cells are primed in the VdLN, exit into the blood where they are detectable by immune monitoring assays, then re-enter the inflamed vaccination site and VdLN, where they respond to vaccine-derived peptide with cytotoxic killing, chemokine and cytokine production, dysfunction and apoptosis. Peptide/IFA vaccination sites contain supraphysiological amounts of antigen; 1 mg/ml (~ 1 mM) of nonamer peptide in our animal model and in many human cancer vaccine trials. Moreover, these peptides are often optimized, more immunogenic variants of the native peptides presented on tumor cells. Thus, peptide/IFA-based vaccination sites may outcompete tumor sites for T cell recognition, chemokine production, T cell accumulation and tissue destruction.

In summary, our findings may help to explain the typically limited clinical benefit of antigen-specific $CD8^+$ T cells induced by a widely used class of cancer vaccines. The recognition that persistent antigen at vaccination sites induces strong sequestration and subsequent dysfunction and deletion of vaccination-induced T cells directly points to desired characteristics of new classes of vaccines based on non-persistent and rapidly biodegradable vaccine adjuvants.

MATERIALS AND METHODS

Animal studies

Animal experiments performed in this study were approved by the Institutional Animal Care and Use Committee (IACUC) of the University of Texas MD Anderson Cancer Center.

Mice and tumor cells

Pmel-1 TCR transgenic mice on a C57BL/6 background (The Jackson Laboratory, Bar Harbor, ME) were crossed with CD90.1 congenic mice to yield pmel-$1^{+/-}$ × CD90.$1^{+/-}$ mice (hereafter referred to as pmel-1 mice). C57BL/6J-Tyr-2J/J Albino mice, OT-I and OT-II TCR transgenic mice, HLA-A0201-Tg, B cell KO (IgH), CD4 KO, IFN-γ KO and FasL KO mice were purchased from The Jackson Laboratory. Animal experiments were approved by the University of Texas M.D. Anderson Institutional Animal Care and Use Committee (IACUC). B16.F10 is an H-2D^{b+}gp100^{+} spontaneous C57BL/6 melanoma obtained from the National Cancer Institute tumor repository and maintained in RPMI 1640 with 10% heat-inactivated FBS, 0.03% L-glutamine, 100 μg ml^{-1} streptomycin, and 100 μg ml^{-1} penicillin (Invitrogen). B16.white is a gp100^{+}, non-pigmented B16 variant[23].

Transduction of pmel-1 T Cells

Retroviral supernatant production and T cell transduction was performed as previously detailed[23]. In brief, splenocytes from pmel-1 mice were cultured in X-Vivo-15 (Lonza) with Normocin (Invivogen), 500 IU/ml rhIL-2 (Novartis), and 0.1 μg/ml anti-mouse CD3 (clone 2C11; BD Biosciences). After 22–24 h, retrovirus encoding enhanced firefly luciferase (v-effLuc) was added at an MOI of 5 in the presence of 1.6 μg ml^{-1} polybrene (Sigma) and 1 μg ml^{-1} Lipofectamine 2000 (Invitrogen) and spinfected at 2000 rpm for 2 h at 30°C. The following d cells were washed and further expanded in Alpha-MEM with 10% FBS, Normocin, and 200 IU ml^{-1} rhIL-2 for 3 d, and sorted using eGFP marker by FACSVantage (BD Biosciences) followed by 48 h in vitro expansion prior to injection.

Peptide vaccination

The synthetic, high-affinity H-2D^{b}-restricted heteroclitic mouse $gp100_{25–33}$ peptide (KVPRNQDWL), H-2K^{b}-restricted chicken ovalbumin $OVA_{257-264}$ (SIINFEKL) and H-2IA^{b}-restricted $OVA_{323–339}$ (ISQAVHAAHAEINEAGR) were purchased from Peptides International at a purity > 95%. Mice received 1000 naive pmel-1 T cells *i.v.* and were vaccinated with two separate s.c. injections at the base of the tail or in each flank with 100 μl of either saline or saline/incomplete Freund's adjuvant (IFA) emulsion (1:1 v/v), each containing 100 μg of $hgp100_{25-33}$ or 50μg of $OVA_{257-264}$ or $OVA_{323-339}$. For imaging studies, C57BL/6J-Tyr-2J/J Albino mice were injected subcutaneously (s.c.) on the shaved back with 3×10^{5} B16.white cells to prevent photon absorption by skin and tumor pigment[23]. Seven d later, 1×10^{6} eGFP-sorted, v-effLuc-transduced pmel-1 T cells were injected i.v. Mice were vaccinated at the indicated d at the posterior and/or anterior flanks with 2 injections of 100 μl of water/incomplete Freund's adjuvant (IFA) or saline/montanide emulsions or PBS containing 100 μg of $hgp100_{25-33}$ peptide, or saline/IFA without peptide as indicated and with or without micrograms of anti-CD40 mAb s.c. and 50 mg of Imiquimod cream 5% (Aldara, Fougera) applied on the vaccination site on d 0 and 2 after vaccination. In addition, we injected 100,000 IU human rIL-2 protein, i.p. (TECIN, Hoffman LaRoche Inc.), once on the d of vaccination and twice a d on the 2 following d. Supernatants from tumor and vaccination site homogenates were analyzed using Luminex kit according to manufacturers' protocol (Millipore). Mice were infected i.v. with 1×10^{6} PFU of VSV-gp100 or VSV.OVA at the indicated d. Tumors were measured with calipers, and the

products of perpendicular diameters were recorded. Mice were sacrificed when tumors reached 200 mm^2 or became ulcerated or mice became moribund.

In vivo bioluminescence imaging

Bioluminescence imaging was performed with a cooled CCD camera mounted in a light-tight specimen box (IVIS 200®, Xenogen Cranbury, New Jersey). For in vivo imaging, animals were given 150 mg/kg of d-luciferin substrate (Caliper Life Sciences, Hopkinton, Massachusetts) i.p.,, anesthetized with 1–% isoflurane and imaged 8 min after d-luciferin injection). Regions of interest from displayed images were designated and quantified as total photon counts or photon s^{-1} (represented by color bars) using Living Image® software (Xenogen, Cranbury, New Jersey).

Transfer experiment

B6 mice were vaccinated either with hgp100 in IFA s.c. with pmel.1 i.v. (donors), hgp100 in IFA *alone* (gp100 recipients) or saline in IFA *alone* (control recipients). Two d later, $CD8^+CD90.1^+CD44^{high}$ cells FACS-sorted from draining lymph nodes of 10 donor mice were transferred into 5 gp100 and control recipients each. Twenty-eight d later, all recipients were boosted with 1×10^6 pfu of VSV.gp100 i.v. and tail bled on indicated d for analysis by flow cytometry.

Tissue preparation

Mice were sacrificed by CO_2 inhalation. PBMC were collected by tail-bled or cardiac puncture. Spleens, lymph nodes, skin sections from vaccination sites and tumors were harvested and stored in cold PBS (Life Technologies). Single cell suspensions were prepared in PBS with 10% FCS, 2 Mm EDTA (Sigma-Aldritch) by mashing tissue against surface of 40μm cell strainer using a plunger of 3ml syringe (Becton Dickinson). RBCs were removed using a hypotonic lysis buffer (StemCell Technologies). Skin sections were minced using surgical blade (Becton Dickinson) and digested with collagenase (Sigma-Aldrich) for 3 h at 37 °C, and then were passed through 18 gauge syringe (Becton Dickinson) and filtered using 40 μm cell strainer (BD Falcon). Mice were tail-bled on the indicated time point.

Antibody staining and FACS analysis

Intracellular IFN-γ staining was performed using the cytofix/cytoperm kit (BD Biosciences) according to the manufacturer's recommendation after 4 h of stimulation with 1 μM $mgp100_{25\text{-}33}$ peptide and using 1/800 dilution of anti-IFNγ-PE mAb (clone: XMG1.2). Annexin V binding assay was performed on unfixed cells with an Annexin V-FITC staining kit according to the manufacturers' instruction (BD Biosciences). Antibodies utilized for staining included anti-CD8 (clone 53-6.7), anti-CD90.1 (clone HIS51), anti-Vβ5 (clone MR9-4), anti-CD44 (clone IM7), anti-TNFα (clone MP6-XT22), anti-CD152 (clone UC10-4B9), anti-CD95 Fas (clone 15A7), anti-CD11c (clone HL3), anti-CD11b (clone M1/70), anti-Ly-6G and Ly-6C (clone RB68C5), anti-CD19 (clone MB19-1) anti-CD127 (clone A7R34), anti-KLRG1 (clone 2F1), anti-Tim-3 (clone 8B.2C12), anti-CCR7 (clone 4B12), anti-CD62L (clone MEL-14), anti-LAG-3 (clone C9B7W), anti-Ki67 (clone SOIA15) from eBioscience, anti-CD178 FasL (clone KAY10), anti-Ly-6C (clone AL-21),

anti-Vα2 (clone B20.1) from BD Biosciences, anti-PD-L1 (10F.9G2), anti-PD1 (clone RMPI.30), anti-CXCR3 (clone CXCR3-173), anti-Bcl-2 (clone BCL/10C4) from Biolegend, anti-Bcl-xL (clone 54H6) from Cell Signaling. .

Gene expression profiling

Mice received 1, 000 pmel-1 T cells i.v. and s.c. vaccination with gp100/saline or gp100/IFA followed by covax. Six and 21 d later, Splenocyte suspensions were RBC-lysed 6 and 21 d later and pmel-1 T cells were column-sorted using magnetic microbeads (Miltenyi Biotech) coated with CD90.1 mAb, followed by FACS-sorting using CD8 and CD90.1. Total RNA was extracted using the RNAqueous kit (Ambion, Austin, TX) on d 6 and 21 after vaccination with gp100/IFA+covax or gp100/saline+covax. After confirmation of RNA quality using a Bioanalyzer 2100 instrument (Agilent), 100 ng or less of total RNA was amplified and biotin-labeled through a two-round Eberwine procedure using MessageAmp II and Illumina TotalPrep RNA Amplification kits (Ambion), and hybridized to Illumina Ref-6 version 2 mouse whole-genome arrays. Processing of bead-level data was by methods previously described. Significance testing for differentially-expressed probes was by the Wilcoxon rank-sum test applied to individual processed bead values, with false-discovery rate significance values (q) determined by the method of Benjamini and Hochberg[57]. Hierarchical clustering and heat mapping used Cluster and Treeview software from Eisen et al.[58] Gene set analysis applied gene set enrichment analysis (GSEA)[59] and the hypergeometric distribution test[60] to gene sets from mSigDB and individual literature sources.

Statistical analysis

All results are expressed as (mean ± s.e.m). Animal and sample group size was (n=5) unless otherwise indicated. Data were analyzed using paired or non-pared two-tailed t-test where applicable and differences were determined significant at (P<0.05). All experiments were repeated at least once with comparable results. We applied nonparametric Kruskal-Wallis with Dunn's multiple comparison test to the time duration from tumor injection until the tumor size reached ≥200mm^2 to determine statistical significance of differences in tumor size measurements between treatment groups.

Supplementary Material

Refer to Web version on PubMed Central for supplementary material.

ACKNOWLEDGEMENTS

The authors wish to thank G. Lizee, N. Martin-Orozco and J. Khalili for their helpful comments on this manuscript. This work was supported by the National Institutes of Health (NIH) grants R01 1CA143077 (WWO) and P01 CA128913 (PH/WWO) and a Melanoma Research Alliance Established Investigator Award (WWO).

References

1. Schwartzentruber DJ, et al. gp100 peptide vaccine and interleukin-2 in patients with advanced melanoma. N Engl J Med. 2011; 364:2119–2127. [PubMed: 21631324]

2. Kantoff PW, et al. Sipuleucel-T immunotherapy for castration-resistant prostate cancer. N Engl J Med. 2010; 363:411–422. [PubMed: 20818862]
3. Kenter GG, et al. Vaccination against HPV-16 oncoproteins for vulvar intraepithelial neoplasia. N.Engl.J.Med. 2009; 361:1838–1847. [PubMed: 19890126]
4. Schuster SJ, et al. Vaccination with patient-specific tumor-derived antigen in first remission improves disease-free survival in follicular lymphoma. J Clin Oncol. 2011; 29:2787–2794. [PubMed: 21632504]
5. Lizee G, et al. Harnessing the Power of the Immune System to Target Cancer. Annual review of medicine. 2012
6. Rosenberg SA, et al. Tumor Progression Can Occur despite the Induction of Very High Levels of Self/Tumor Antigen-Specific CD8+ T Cells in Patients with Melanoma. J.Immunol. 2005; 175:6169–6176. [PubMed: 16237114]
7. Rosenberg SA, Yang JC, Restifo NP. Cancer immunotherapy: moving beyond current vaccines. Nat.Med. 2004; 10:909–915. [PubMed: 15340416]
8. Smyth MJ, Dunn GP, Schreiber RD. Cancer immunosurveillance and immunoediting: the roles of immunity in suppressing tumor development and shaping tumor immunogenicity. Adv Immunol. 2006; 90:1–50. [PubMed: 16730260]
9. Lizee G, Radvanyi LG, Overwijk WW, Hwu P. Improving antitumor immune responses by circumventing immunoregulatory cells and mechanisms. Clin.Cancer Res. 2006; 12:4794–4803. [PubMed: 16914564]
10. Bonhoure F, Gaucheron J. Montanide ISA 51 VG as adjuvant for human vaccines. J Immunother. 2006; 29:647–648.
11. Reinhardt RL, Bullard DC, Weaver CT, Jenkins MK. Preferential accumulation of antigen-specific effector CD4 T cells at an antigen injection site involves CD62E-dependent migration but not local proliferation. J Exp Med. 2003; 197:751–762. [PubMed: 12629067]
12. Redmond WL, Sherman LA. Peripheral tolerance of CD8 T lymphocytes. Immunity. 2005; 22:275–284. [PubMed: 15780985]
13. Aichele P, Brduscha-Riem K, Zinkernagel RM, Hengartner H, Pircher H. T cell priming versus T cell tolerance induced by synthetic peptides. J Exp Med. 1995; 182:261–266. [PubMed: 7540654]
14. Toes RE, Offringa R, Blom RJ, Melief CJ, Kast WM. Peptide vaccination can lead to enhanced tumor growth through specific T-cell tolerance induction. Proc.Natl.Acad.Sci.U.S.A. 1996; 93:7855–7860. [PubMed: 8755566]
15. Bijker MS, et al. Superior induction of anti-tumor CTL immunity by extended peptide vaccines involves prolonged, DC-focused antigen presentation. Eur.J.Immunol. 2008; 38:1033–1042. [PubMed: 18350546]
16. Health, N.I.o. Montanide and cancer. 2011. http://www.clinicaltrials.gov/ct2/results?term=montanide+cancer
17. Overwijk WW, et al. gp100/pmel 17 is a murine tumor rejection antigen: induction of “self”-reactive, tumoricidal T cells using high-affinity, altered peptide ligand. J.Exp.Med. 1998; 188:277–286. [PubMed: 9670040]
18. Overwijk WW, et al. Tumor Regression and Autoimmunity after Reversal of a Functionally Tolerant State of Self-reactive CD8+ T Cells. J Exp Med. 2003; 198:569–580. [PubMed: 12925674]
19. Overwijk WW, et al. Immunological and Antitumor Effects of IL-23 as a Cancer Vaccine Adjuvant. J.Immunol. 2006; 176:5213–5222. [PubMed: 16621986]
20. Bijker MS, et al. CD8+ CTL priming by exact peptide epitopes in incomplete Freund’s adjuvant induces a vanishing CTL response, whereas long peptides induce sustained CTL reactivity. J.Immunol. 2007; 179:5033–5040. [PubMed: 17911588]
21. Smith RT, Bridges RA. Immunological unresponsiveness in rabbits produced by neonatal injection of defined antigens. J Exp Med. 1958; 108:227–250. [PubMed: 13563758]
22. Critchfield JM, et al. T cell deletion in high antigen dose therapy of autoimmune encephalomyelitis. Science. 1994; 263:1139–1143. [PubMed: 7509084]

23. Rabinovich BA, et al. Visualizing fewer than 10 mouse T cells with an enhanced firefly luciferase in immunocompetent mouse models of cancer. Proc.Natl.Acad.Sci.U.S.A. 2008; 105:14342–14346. [PubMed: 18794521]
24. Hambach L, Aghai Z, Pool J, Kroger N, Goulmy E. Peptide length extension skews the minor HA-1 antigen presentation toward activated dendritic cells but reduces its presentation efficiency. J Immunol. 185:4582–4589. [PubMed: 20855877]
25. Janicki CN, Jenkinson SR, Williams NA, Morgan DJ. Loss of CTL function among high-avidity tumor-specific CD8+ T cells following tumor infiltration. Cancer Res. 2008; 68:2993–3000. [PubMed: 18413769]
26. Riquelme E, Carreno LJ, Gonzalez PA, Kalergis AM. The duration of TCR/pMHC interactions regulates CTL effector function and tumor-killing capacity. Eur J Immunol. 2009; 39:2259–2269. [PubMed: 19637198]
27. Zehn D, Lee SY, Bevan MJ. Complete but curtailed T-cell response to very low-affinity antigen. Nature. 2009; 458:211–214. [PubMed: 19182777]
28. Muraoka D, et al. Peptide vaccine induces enhanced tumor growth associated with apoptosis induction in CD8+ T cells. J Immunol. 2010; 185:3768–3776. [PubMed: 20733202]
29. Refaeli Y, Van Parijs L, Alexander SI, Abbas AK. Interferon gamma is required for activation-induced death of T lymphocytes. J.Exp.Med. 2002; 196:999–1005. [PubMed: 12370261]
30. Gabrilovich DI, Ostrand-Rosenberg S, Bronte V. Coordinated regulation of myeloid cells by tumours. Nat Rev Immunol. 2012; 12:253–268. [PubMed: 22437938]
31. Yang S, Hodge JW, Grosenbach DW, Schlom J. Vaccines with enhanced costimulation maintain high avidity memory CTL. J Immunol. 2005; 175:3715–3723. [PubMed: 16148117]
32. Ugel S, et al. Immune tolerance to tumor antigens occurs in a specialized environment of the spleen. Cell reports. 2012; 2:628–639. [PubMed: 22959433]
33. van Heijst JWJ, et al. Recruitment of Antigen-Specific CD8+ T Cells in Response to Infection Is Markedly Efficient. Science. 2009; 325:1265–1269. [PubMed: 19729659]
34. Schoenberger SP, Toes RE, van der Voort EI, Offringa R, Melief CJ. T-cell help for cytotoxic T lymphocytes is mediated by CD40-CD40L interactions. Nature. 1998; 393:480–483. [PubMed: 9624005]
35. Kedl RM, et al. CD40 stimulation accelerates deletion of tumor-specific CD8(+) T cells in the absence of tumor-antigen vaccination. Proc Natl Acad Sci U S A. 2001; 98:10811–10816. [PubMed: 11526222]
36. Ahonen CL, et al. Combined TLR and CD40 triggering induces potent CD8+ T cell expansion with variable dependence on type I IFN. J Exp Med. 2004; 199:775–784. [PubMed: 15007094]
37. Ly LV, et al. Peptide vaccination after T-cell transfer causes massive clonal expansion, tumor eradication, and manageable cytokine storm. Cancer Res. 2010; 70:8339–8346. [PubMed: 20940397]
38. Verdeil G, Marquardt K, Surh CD, Sherman LA. Adjuvants targeting innate and adaptive immunity synergize to enhance tumor immunotherapy. Proc Natl Acad Sci U S A. 2008; 105:16683–16688. [PubMed: 18936481]
39. Wojciechowski S, et al. Bim mediates apoptosis of CD127(lo) effector T cells and limits T cell memory. Eur J Immunol. 2006; 36:1694–1706. [PubMed: 16761315]
40. Wojciechowski S, et al. Bim/Bcl-2 balance is critical for maintaining naive and memory T cell homeostasis. J Exp Med. 2007; 204:1665–1675. [PubMed: 17591857]
41. Hildeman DA, et al. Activated T cell death in vivo mediated by proapoptotic bcl-2 family member bim. Immunity. 2002; 16:759–767. [PubMed: 12121658]
42. Matsushita H, et al. Cancer exome analysis reveals a T-cell-dependent mechanism of cancer immunoediting. Nature. 2012; 482:400–404. [PubMed: 22318521]
43. Gajewski TF, Fuertes M, Spaapen R, Zheng Y, Kline J. Molecular profiling to identify relevant immune resistance mechanisms in the tumor microenvironment. Curr Opin Immunol. 2011; 23:286–292. [PubMed: 21185705]
44. Wherry EJ. T cell exhaustion. Nat Immunol. 2011; 12:492–499. [PubMed: 21739672]

45. Jin HT, et al. Cooperation of Tim-3 and PD-1 in CD8 T-cell exhaustion during chronic viral infection. Proc Natl Acad Sci U S A. 2010; 107:14733–14738. [PubMed: 20679213]
46. Wherry EJ, et al. Molecular signature of CD8+ T cell exhaustion during chronic viral infection. Immunity. 2007; 27:670–684. [PubMed: 17950003]
47. den Boer AT, et al. Longevity of antigen presentation and activation status of APC are decisive factors in the balance between CTL immunity versus tolerance. J Immunol. 2001; 167:2522–2528. [PubMed: 11509591]
48. den Boer AT, et al. The tumoricidal activity of memory CD8+ T cells is hampered by persistent systemic antigen, but full functional capacity is regained in an antigen-free environment. J.Immunol. 2004; 172:6074–6079. [PubMed: 15128791]
49. Rezvani K, et al. Repeated PR1 and WT1 peptide vaccination in Montanide-adjuvant fails to induce sustained high-avidity, epitope-specific CD8+ T cells in myeloid malignancies. Haematologica. 2010; 96:232–240.
50. Speiser DE, Romero P. Toward improved immunocompetence of adoptively transferred CD8+ T cells. J Clin Invest. 2005; 115:1467–1469. [PubMed: 15931384]
51. Appay V, et al. New generation vaccine induces effective melanoma-specific CD8+ T cells in the circulation but not in the tumor site. J Immunol. 2006; 177:1670–1678. [PubMed: 16849476]
52. Kenter GG, et al. Phase I immunotherapeutic trial with long peptides spanning the E6 and E7 sequences of high-risk human papillomavirus 16 in end-stage cervical cancer patients shows low toxicity and robust immunogenicity. Clin.Cancer Res. 2008; 14:169–177. [PubMed: 18172268]
53. Speetjens FM, et al. Induction of p53-specific immunity by a p53 synthetic long peptide vaccine in patients treated for metastatic colorectal cancer. Clin Cancer Res. 2009; 15:1086–1095. [PubMed: 19188184]
54. Leffers N, et al. Immunization with a P53 synthetic long peptide vaccine induces P53-specific immune responses in ovarian cancer patients, a phase II trial. Int J Cancer. 2009; 125:2104–2113. [PubMed: 19621448]
55. Yamshchikov GV, et al. Evaluation of peptide vaccine immunogenicity in draining lymph nodes and peripheral blood of melanoma patients. Int J Cancer. 2001; 92:703–711. [PubMed: 11340576]
56. Schaefer JT, et al. Dynamic changes in cellular infiltrates with repeated cutaneous vaccination: a histologic and immunophenotypic analysis. J Transl Med. 2010; 8:79. [PubMed: 20727190]
57. Benjamini Y, Hochberg Y. Controlling the false discovery rate: a practical and powerful approach to multiple testing. J Roy Stat Soc B. 1995; 57:289–300.
58. Eisen MB, Spellman PT, Brown PO, Botstein D. Cluster analysis and display of genome-wide expression patterns. Proc Natl Acad Sci U S A. 1998; 95:14863–14868. [PubMed: 9843981]
59. Subramanian A, et al. Gene set enrichment analysis: a knowledge-based approach for interpreting genome-wide expression profiles. Proc Natl Acad Sci U S A. 2005; 102:15545–15550. [PubMed: 16199517]
60. Jakt LM, Cao L, Cheah KS, Smith DK. Assessing clusters and motifs from gene expression data. Genome Res. 2001; 11:112–123. [PubMed: 11156620]

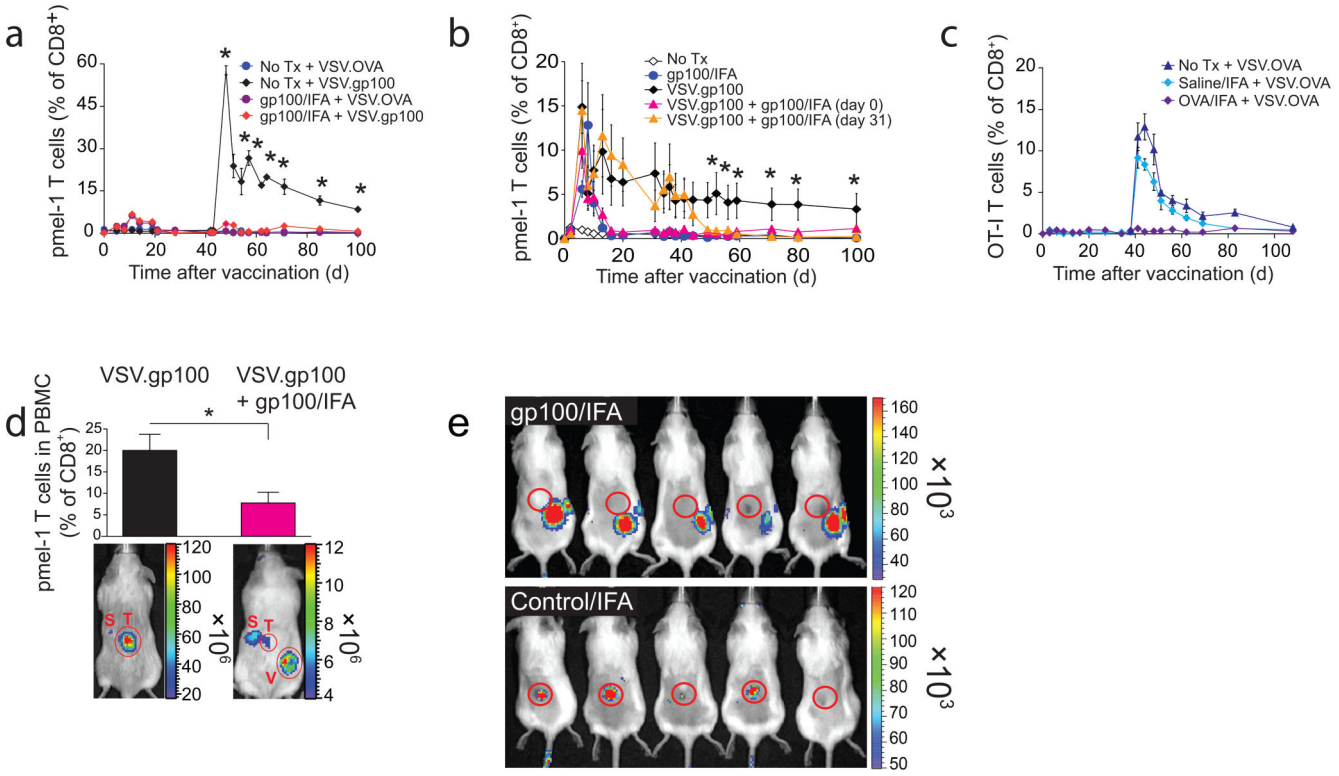

Figure 1.

Vaccination with gp100 in IFA induces CD8$^+$ T cell priming followed by hyporesponsiveness. (**a**) Mice received gp100-specific CD90.1$^+$ pmel-1 T cells and gp100/IFA s.c. or saline/IFA control vaccination or were left unvaccinated. On day 42, mice were boosted with VSV.gp100 or control VSV.OVA. Levels of CD90.1$^+$ pmel-1 T cells in blood (mean ± s.e.m.) are shown. (**b**) Mice received pmel-1 T cells and VSV.gp100 i.v. on day 0 and/or s.c. vaccination with gp100/IFA on day 0 or 31. Levels of pmel-1 T cells in blood are shown. (**c**) Mice were vaccinated with s.c. OVA/IFA or saline/IFA and boosted on day 36 with VSV.OVA. OVA tetramer$^+$ endogenous CD8$^+$ T cells in blood are shown. (**d**) Albino C57BL/6 mice bearing 7 d, palpable, B16 melanoma were vaccinated with gp100/IFA *s.c.* and/or VSV.gp100 *i.v.* and received 1 × 10^6 v-effLuc-transduced pmel-1 T cells *i.v.*, followed by 3 d of IL-2. Mean number of pmel-1 T cells in blood (**top**) and representative imaged mice 4 d after vaccination (**bottom**) photons s^{-1} are shown. T, tumor; V, gp100/IFA vaccination site; S, spleen. (**e**) Albino C57BL/6 mice bearing 7 d, palpable, B16 melanomas were vaccinated with gp100/IFA or saline/IFA *s.c.* and received v-effLuc-transduced pmel-1 T cells *i.v.* and 3 d of IL-2. Pmel-1 T cells were visualized on day 7. Circles indicate location of *s.c.* B16 tumor. Color bars represent photons s$^{-1.}$ Data shown are representative of at least two experiments, each with (n=5 per group per experiment). * P<0.05.

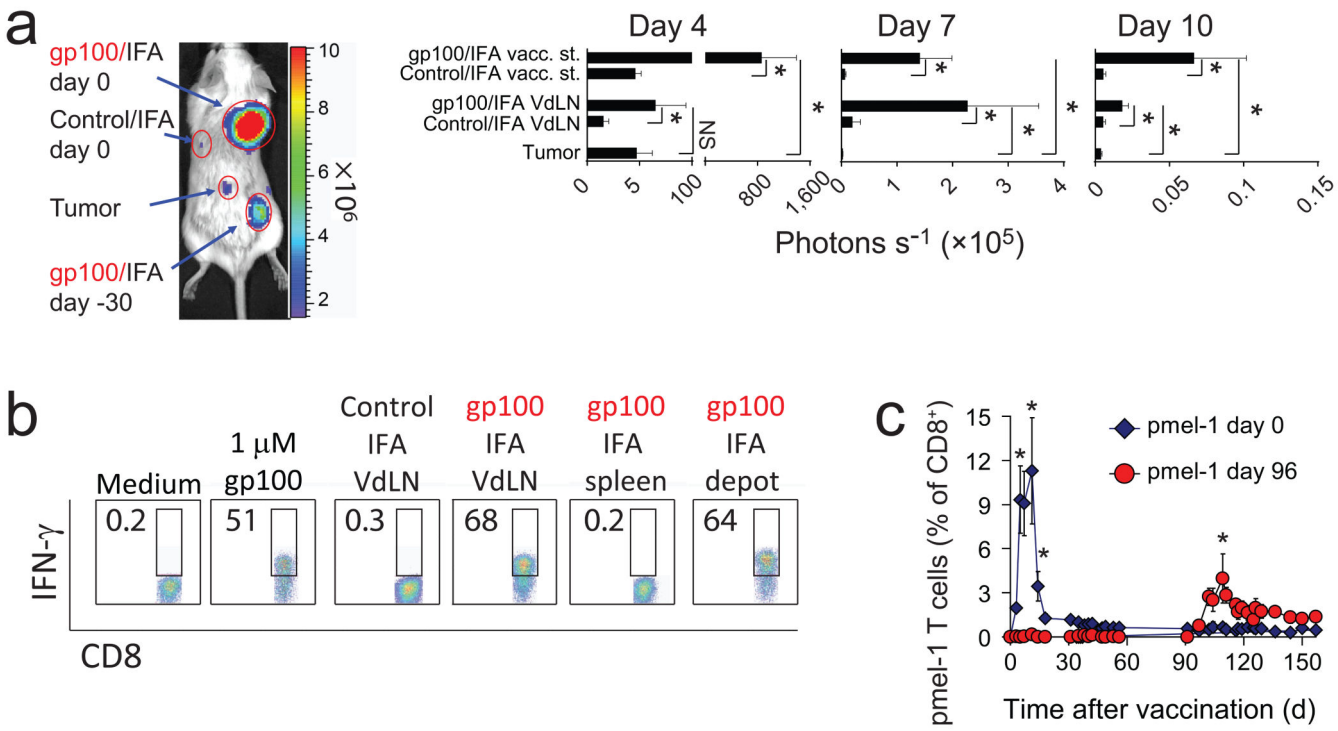

Figure 2.

Vaccination with gp100/IFA induces chronic antigen presentation and T cell sequestration. (**a**) Albino C57BL/6 mice bearing 7 d, palpable s.c. B16 tumors were vaccinated s.c. with gp100/IFA on day 0 or −30 or saline/IFA on day 0 and received 1×10^6 v-effLuc-transduced pmel-1 T cells i.v. followed by 3 d of IL-2. After 4 d, mice were imaged for pmel-1 T cell localization, a representative mouse (photons s^{-1}) is shown. Kinetics of absolute pmel-1 T cell luminescence (mean ± s.e.m., n=5) in different organs/tissues after day 0 vaccination are plotted (**b**) Mice were vaccinated s.c. with gp100/IFA or saline/IFA. After 30 d, vaccine-draining lymph nodes (VdLN), spleen and the vaccine depot itself were removed and VdLN cells, splenocytes, recovered vaccine emulsion or 1 μM of gp100 peptide were added to cultured pmel-1 effector T cells; 4 h intracellular IFN-γ staining in pmel-1 T cells (mean ± s.e.m.) is shown (**c**) Mice were vaccinated with gp100/IFA on day 0, followed by pmel-1 T cells on day 0 or on day 96. Levels of pmel-1 T cells (mean ± s.e.m.) in blood are shown. Data shown are representative of at least two experiments, each with (n=5 per group per experiment). * $P<0.05$

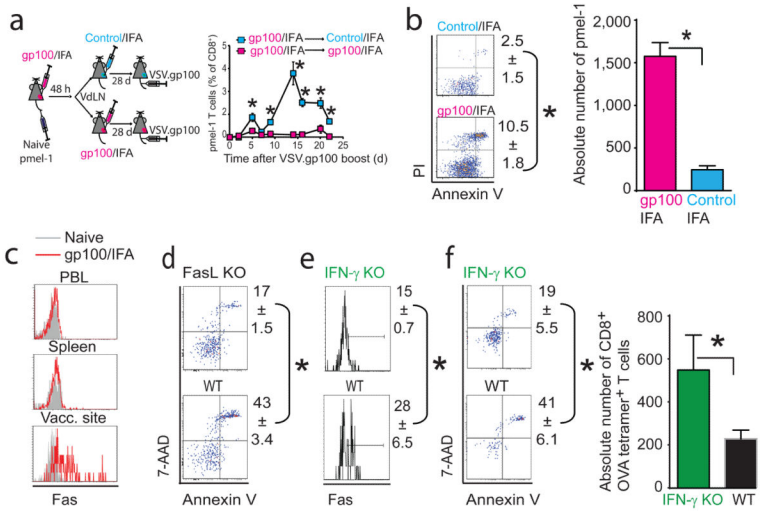

Figure 3.

Vaccination-induced CD8+ T cell apoptosis at the vaccination site is driven by antigen and IFN-γ and requires host FasL. (**a**) Mice received pmel-1 T cells and gp100/IFA s.c. After 48 h, 1000 primed CD44$^+$ CD8$^+$ T cells were sorted from VdLN and transferred i.v. to recipient mice bearing 48 h old s.c. gp100/IFA or saline/IFA vaccine depots. Twenty-eight d later, all recipient mice were boosted with VSV.gp100; subsequent levels of pmel-1 T cells in blood are shown. (**b**) Mice received CD90.1$^+$ pmel-1 T cells and gp100/IFA and saline/IFA vaccination on opposite flanks. 6 d later, apoptotic death of CD90.1$^+$ pmel-1 T cells from VdLN was quantified (mean ± s.e.m., n=10). Absolute number of pmel-1 T cell (mean ± s.e.m., n=5) per VdLN is plotted (**right panel**). (**c**) Fas expression on pmel-1 T cells 6 d after gp100/IFA vaccination. (**d**) C57BL/6 and FasL-KO mice received pmel-1 T cells and gp100/IFA vaccination, 6 d later apoptotic cell death of pmel-1 T cells at the vaccination site was measured by flow cytometry. (**e**) C57BL/6 and IFN-γ-KO mice received OVA/IFA s.c., 6 d later Fas expression and (**f**) apoptotic cell death was measured by gating on endogenous OVA tetramer$^+$CD8$^+$ T cells recovered from the vaccination site; absolute number of CD8$^+$ OVA tetramer$^+$ T cells at vaccination site is also shown. Data are representative of at least two experiments, each with 5 mice per group. * P <0.05

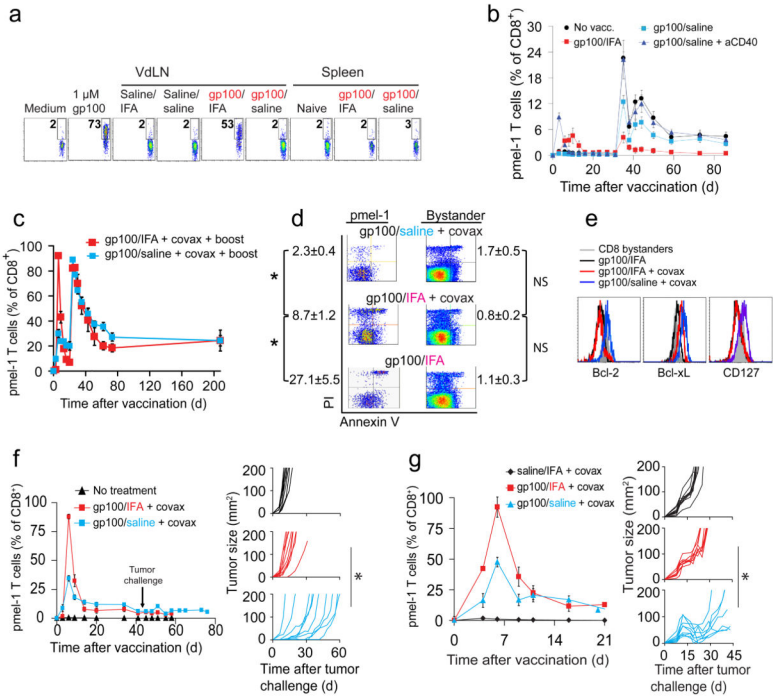

Figure 4.

T cell sequestration and deletion is overcome by vaccination with a short-lived, water-based vaccine formulation (**a**) Mice were vaccinated s.c. with gp100/IFA or saline/IFA. 1×10^5 freshly isolated VdLN cells or splenocytes or 1 μM of gp100 peptide were added to 1×10^5 cultured pmel-1 effector T cells 6 d later. 4 h intracellular IFN-γ staining in pmel-1 T cells is shown. (**b**) Mice received pmel-1 T cells and gp100/IFA or gp100/saline vaccine s.c. and 50 μg anti-CD40 mAb s.c. and were boosted after 31 d with VSV.gp100 i.v; pmel-1 T cells levels (mean ± s.e.m.) in blood are shown. (**c**) Mice received pmel-1 T cells and gp100/IFA or gp100/saline vaccine s.c. and covax (50 μg anti-CD40 mAb s.c., 50 μg imiquimod cream applied on the vaccination site and 3 d of 100,000 IU rhIL-2 i.p.) on d 0 and again but without imiquimod on d 21; pmel-1 T cells levels in blood are shown. (**d**) Mice (n=5) were treated as in (c) and apoptotic cell death in VdLN was measured 6 d later. (**e**) Mice (n=5) were treated as in (c) and 5 d later expression of Bcl-2, Bcl-xL and CD127 in pmel-1 T cells from VdLN was measured by flow cytometry. (**f**) Mice (n=10) received pmel-1 T cells and gp100/IFA or gp100/saline vaccine s.c. and covax on day 0 and B16 tumor challenge on day 41. Shown are levels of pmel-1 T cells in blood (**left panel**) and tumor size for individual mice (**right panels**). (**g**) Mice (n=10) bearing 7 d, palpable s.c. B16 melanoma received pmel-1 T cells and s.c. vaccination with gp100/saline or gp100/IFA and covax on day 0. Shown are pmel-1 T cell levels in blood (**left panel**) and tumor size in individual mice (**right panels**). Data shown are representative of at least two experiments, each with 5 mice per group. * P <0.05, NS (not significant): P>0.05.

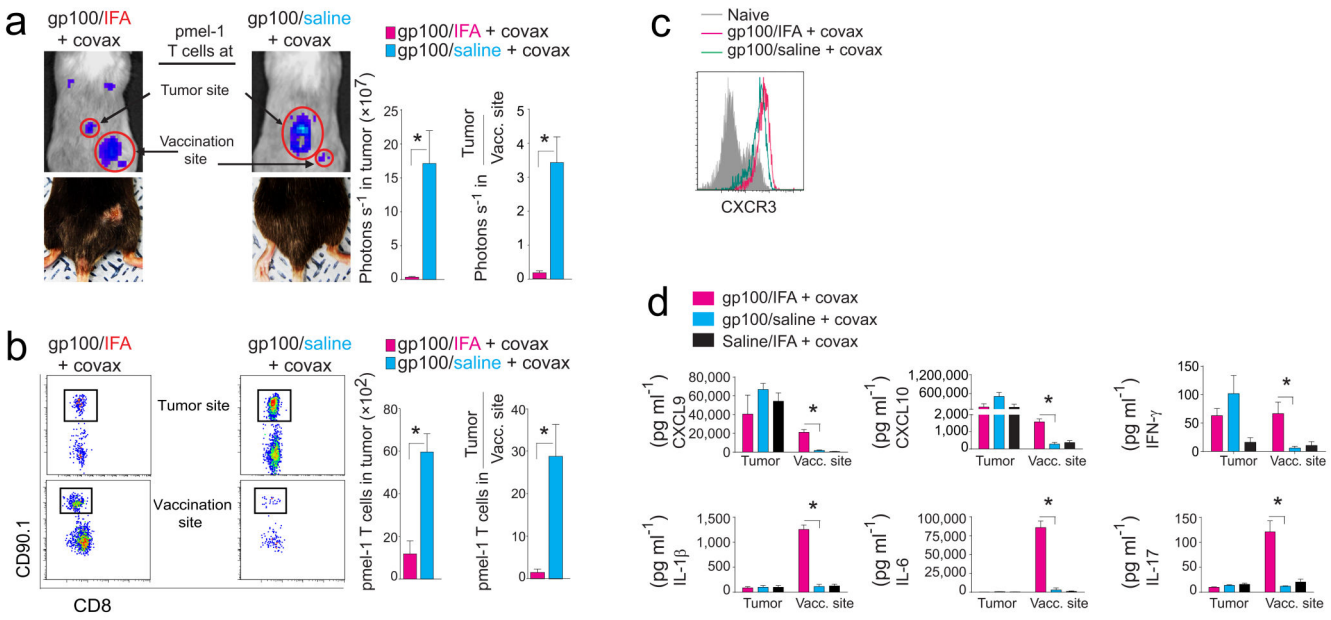

Figure 5.

Vaccination with a short-lived, water-based vaccine formulation allows T cell localization to tumors (**a**) Albino C57BL/6 mice bearing 7 d palpable B16.white melanoma received v-effLuc-transduced pmel-1 effector T cells i.v. and gp100/IFA+covax or gp100/saline+covax. After 7 d, pmel-1 T cells were visualized (**top left panels**) and quantified in tumor and vaccination site. Absolute pmel-1 T cell luminescence (mean ± s.e.m., n=5) in tumor and ratio of pmel-1 T cell luminescence in tumor *vs.* vaccination site (mean ± s.e.m., n=5) are plotted (**right panels**). The graph is representative of three replicate experiments. Vaccination sites of C57BL/6 mice that received pmel-1 and gp100/IFA+covax or gp100/saline+covax s.c. were photographed 31 d after vaccination (**bottom left panels**). (**b**) Mice bearing 7 d palpable B16 melanoma received pmel-1 T cells and gp100/IFA or gp100/saline saline/IFA vaccine s.c. and covax and 6 d later tumor and vaccination sites were excised and levels of pmel-1 T cell infiltration were quantified by flow cytometry. (**c**) CXCR3 expression by pmel-1 T cells in PBL 6 d after vaccination (**d**) Supernatant from tumor and vaccination site homogenates from (**b**) were used to measure cytokine/chemokine concentrations (mean ± s.e.m.). Data shown are representative of three experiments, each with 5 mice per group. * P <0.05, NS (not significant): P>0.05.

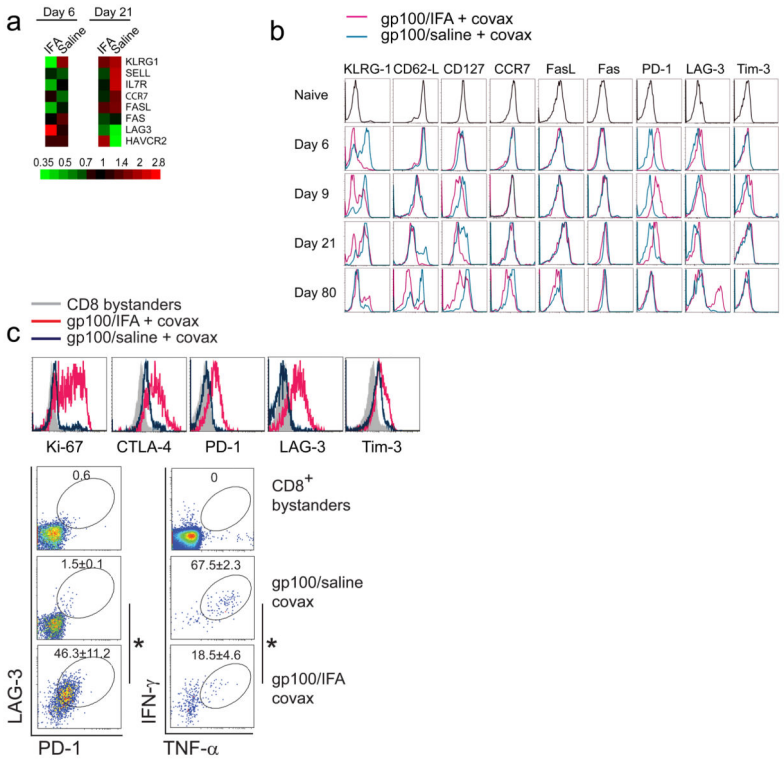

Figure 6.

pmel-1 T cell phenotype after vaccination with gp100/IFA + covax *vs.* gp100/saline + covax. (**a**) Mice bearing 7 d palpable B16 melanoma received pmel-1 T cells and gp100/IFA or gp100/saline saline/IFA vaccine s.c. and covax. Gene expression profiles were measured 6 and 21 d later. (**b**) Expression of indicated molecules in peripheral blood was assessed over time by flow cytometry by gating on $CD8^+CD90.1^+$ pmel-1 T cells. (**c**) Proliferation, expression of inhibitory markers and cytokine production in pmel-1 T cells from VdLN 23 d after vaccination with gp100/IFA *vs.* gp100/saline. * P <0.05